Polycyclic Aromatic Compounds, 34:263–279, 2014

ISSN: 1040-6638 print / 1563-5333 online
DOI: 10.1080/10406638.2014.892887

Photodegradation of Anthracene and Benzo[*a*]anthracene in Polar and Apolar Media: New Pathways of Photodegradation

Vito Librando,[1,2] Giuseppina Bracchitta,[1] Guido de Guidi,[1,2,3] Zelica Minniti,[1,2] Giancarlo Perrini,[1,2] and Alfio Catalfo[1]

[1]Dipartimento di Scienze Chimiche, Università di Catania, Catania, Italy
[2]Research Center for Analysis, Monitoring and Minimization Methods of Environmental Risk Chemical Sciences Building, Catania, IT
[3]Inca-Consorzio Interuniversitario Chimica per l'Ambiente, Marghera (VE), Italy

The photochemical reactions of anthracene and benzo[*a*]anthracene polycyclic aromatic hydrocarbons (PAHs) in polar and apolar solvents (cyclohexane and water/acetonitrile) were studied using spectroscopic and chromatographic techniques. These homogenous photolysis experiments are used as simplified models to compare PAHs photochemistry in water and oil (or oil films). Moreover, these processes were to some extent used as model in literature in order to study those occurring on particulate matter and aerosol surfaces. In both media, new photochemical reaction products were found. Generally, the reaction rate in the polar medium is faster than that in the apolar medium, and the photodegradation quantum yields increase with increasing polarity of the medium. HPLC-absorption/emission analysis confirmed the literature reports that mainly oxygenated photoproducts, such as PAH-hydroxides, were formed. The novelty of this article is that GC-MS data revealed the presence of new photoproducts that have not yet been described. This simplified model system allowed us to characterize the product distribution, thus simplifying the interpretation of the photodegradation mechanism. The identification of new photofragmentation paths, originating by irradiation of primary PAH photoproducts, may suggest an innovative way of remediation triggered by light.

Key Words: anthracene (AN), benzo[*a*]anthracene (BaAN), particulate matter, photodegradation, polycyclic aromatic hydrocarbon (PAH)

Received 5 October 2013; accepted 6 February 2014.
Address correspondence to Vito Librando, Dipartimento di Scienze Chimiche, Università di Catania, Viale Andrea Doria 6, 95125, Catania, Italy. E-mail: vlibrando@unict.it

INTRODUCTION

PAH photolysis in bulk phases (air, water, and oil) are typically homogeneous reactions. Moreover, PAH photolysis in interfacial phases of fly ashes, diesel soot, and wood smoke particles in known to be the main process in particulate matter; all these processes are heterogeneous reactions (1,2). Solar UVA-B radiation initiates a photochemical reaction which represents the main degradation process for chemicals in both bulk and interface regions. Polycyclic aromatic hydrocarbons (PAHs) are often associated with solid particulate matter (3–5). PAHs photolysis can proceed in different ways depending on the surroundings. Thus, PAH photolysis in vapor phase can include direct and indirect (i.e., OH mediated) processes.

PAHs can absorb sunlight (300–420 nm) and are thermally stable due to their delocalized π-electron clouds and large resonance energies. On the other hand, they can be photolyzed via different reaction paths:

a. Reactions that occur in the homogeneous gas phase proceed more slowly than those occurring on surfaces via heterogeneous processes. In this case, the rate-determining factor is the concentration of compounds on the surface (6). PAHs can also be washed away in aquatic systems (7) resulting in increased hydrophilicity, where the compounds are photodegraded (8).

b. The homogenous photoreactions, kinetics, and reaction products of PAHs were studied both in aqueous (9,10) and nonaqueous environment (11–13). Photolysis in these bulk phases is driven by two main factors: UV radiation and ozonation (9,10). Many UV photolysis products are more toxic than the parent compounds (14). Some reports describe photoproduction of PAH derivatives with light sources that contain high levels of UVC ($<$280 nm). This component, however, is not present in sunlight (1). Generally, UV photolysis in homogenous phases results in ring opening of PAHs by photochemically generated radicals (2,15), analogously to what is found in other pollutants (5,16).

c. Films of water (for example, on wood smoke particles and aerosol particles) and the composition of particulate matter affect the way that organic compounds are processed in the atmosphere (17). Various atmospheric compounds can be contained in particulate matter (PM) and interact with water and support a variety of heterogeneous reactions (7,18).

This article focuses on the photochemical transformation of two PAHs. Benzo[a]anthracene (BaAN) and anthracene (AN) were studied on homogeneous solutions and points out the value of contrasting the photochemistry in water and oil (that can be extended to oil films, i.e., an apolar layer). Indeed, because the photochemical reaction of PAHs adsorbed to particles could also

occur in an organic layer surrounding the particle core, irradiation of the compound in an organic solvent could roughly simulate in laboratory the direct photolytic pathways of pollutant degradation, as described in the literature (12). Thus, these compounds were studied by irradiating the pollutants in organic and aqueous solvents. Cyclohexane, a relatively inert solvent, was used to further simplify the photoreactivity scheme. These photodegradation simulations offer a reasonable approximation and provide good yields of the photoproducts (12) and can suggest an innovative way of remediation triggered by light.

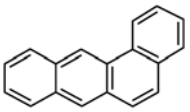

benzo[*a*]anthracene (BaAN)

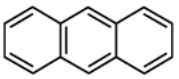

anthracene (AN)

MATERIALS AND METHODS

Reagents

The PAHs, benzo[*a*]anthracene (BaAN), anthracene (AN), and pyrene-d_{10} (internal standard, Py-d_{10}), were obtained from Sigma (Milano), and some other standards were obtained from J. T. Baker (New Jersey) and Chiron AS (Chemical Research 2000 Srl, Roma). Cyclohexane, acetonitrile (ACN), methanol (MeOH), and water were HPLC grade. All other chemicals were reagent grade.

Irradiation Conditions

All samples volume was of 3 ml and a concentration of 4.4 μM BaAN and 20 μM AN in H_2O/ACN (70/30), as well as of 50 μM BaAN and 165 μM AN in cyclohexane, was used. Irradiation was performed in cuvette (optical length, 1 cm) using a Rayonet photochemical reactor, model RPR-100, (maintained at 35°C with a thermostat) equipped with sixteen black light phosphorus lamps (RPR-3500 Å) that emits in the 310–390 nm range, with a maximum intensity at 350 nm. A "merry-go-round" irradiation apparatus (model RMA-500) was used to ensure that all parallel samples received equal radiation. The fluence rate at the irradiation position was approximately 1300 μW/cm^2 as measured by a radiometer (Spectroline, Model DM-365X) equipped with an UVA sensitive sensor (DM-365X) with a spectral range of 320–400 nm. More accurate

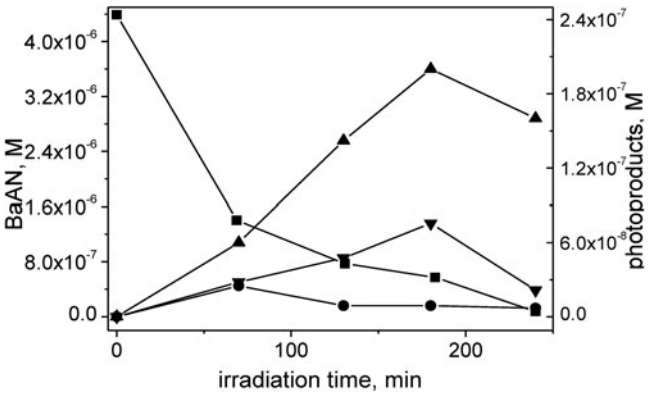

Figure 1: UVA induced photolysis of 4.4 μM BaAN (-■-) in H_2O/ACN (70/30) at various irradiation times; I (-▲-), II (-▼-), III (-●-). HPLC data.

light measurements by ferric oxalate actinometry, carried out by taking into account the integrated area of absorbed light in the 310–390 range of the black light lamps, showed that the incident photon flux on the irradiated solutions in quartz cuvettes (optical length, 1 cm) was 3.9×10^{16} quanta $s^{-1}cm^{-3}$. More details about the experimental procedures of irradiation and light intensity measurements have been described previously (19–21).

Quantum Yield

The quantum yield (φ) of the investigated processes (PAH photodegradation and the formation of their photoproducts, generally indicated as $\boldsymbol{X}$) can be calculated from the initial rate of each process, based on the following Equation (1)):

$$\frac{d[X]}{dt} = \frac{\varphi F I}{V}. \tag{1}$$

$F = 1–10^{-\bar{A}}$ represents the fraction of light absorbed by the PAH. $\bar{A}$ is the mean absorbance of the PAH overlapping the emission range of the black light lamps. In this case, data corrected for $\bar{A}$, fit the absorption spectrum of the compound with that of the lamp only in the overlapping region. Thus, the resulting fraction of light absorbed (F) by the sample represents the exact correction factor in the quantum yield calculus (see Figure 1 in supplementary data). I is the measured light intensity (mol of photons min^{-1}) and V is the volume of the irradiated sample. To calculate photoproducts quantum yields, the determination of their absolute formation rates was achieved with analytical standards to calibrate the instruments.

Analytical Instrumentation

UV–VIS absorption spectra were recorded on a Jasco V-560 spectrophotometer. Emission spectra were obtained on a Spex Fluorolog-2 (Mod F-111) in order to optimize HPLC fluorescence detection of PAHs. The HPLC analyses of PAH and its photoproducts were performed on a PerkinElmer chromatograph (Series 200 LC pump) equipped with a UV/VIS detector (785A), fluorescence detector (LC 240) and Interface (950A). GC/MS analyses were performed in splitless mode with a Finningan Trace GC and DSQ (Thermo Electron) equipped with an AS 800 (Fisons) autosampler.

HPLC-UV/Vis-FL of PAHs

For HPLC, 20 μl of sample or standard in aqueous solvent were directly injected in a reverse-phase Lichrospher C-18 (4.6 $\times$ 250). Differently, samples or standards in cyclohexane were first dried with nitrogen and then redissolved in mobile phase before injection. An isocratic mobile phase of water and 80% MeOH (v/v) was used at a flow rate of 1 ml/min (7). PAHs were resolved by changing the excitation/emission wavelengths in the fluorescence detector (FL): 270/390 for the internal standard, Py-d_{10}, 255/385 for BaAN, and 260/398 for AN. Retention times of PAHs and their photoproducts are reported in Tables 1 and 2.

GC-MS of PAHs

GC analyses were performed in electron impact mode (EI; 70 eV) on a J&W DB-5MS (0.25 μm, 30 m $\times$ 0.250 mm) with 1 ml min^{-1} helium carrier gas. Temperatures of the injector and transfer line were 250 and 300°C, respectively, and the thermal program for elution was 70°C, 1 min hold, 70–300°C at 10°C min^{-1}, 1 min hold. Two separate chromatograph runs were used to characterize PAHs and their derivatives by using both scan and Selected Ion Monitoring (SIM) mode. The internal standard Py-d_{10} was used. Sample or standard in cyclohexane were directly injected without further treatment. Differently, sample or standard in aqueous solvent were first dried with nitrogen and then re-dissolved in cyclohexane before injection.

The definitive identification of lower abundance PAH derivatives was achieved using MS measurements (i.e., mass spectral interpretation and literature data).

RESULTS AND DISCUSSION

Kinetics of Photodegradation

The photodegradation of AN and BaAN was followed both by UV visible spectral changes and HPLC at various irradiation times; peak assignment was

Table 1: Quantum yields of photodegradation (φ_{degr}), Inter System Crossing (φ_{ISC}), and singlet oxygen (φ_{Δ}). Retention time (t_r), extinction coefficient (ε), photodegradation rate constants (k_p), reaction rate constants with oxygen (k_{O2}), and half-life ($t_{1/2}$) of BaAN and AN in water/ACN and cyclohexane. Singlet oxygen lifetime (τ) in cyclohexane and in water/ACN.

			water/ACN (70/30)						cyclohexane						
	t_r, min GC	t_r, min HPLC	ε_{338}	φ_{degr}	φ_{ISC} #	φ_{Δ} #	$\tau = 15\ \mu s^{£}$ k_p, s^{-1}	$t_{1/2}$, min	ε_{338}	φ_{degr}	φ_{ISC} #	φ_{Δ} #	k_p, s^{-1}	$t_{1/2}$, min	$\tau = 23\ \mu s^{\$}$ $k_{O2}, Lmol^{1}s^{-1*}$
BaAN	21.0	42.5	3706	4.2×10^{-4}	0.79	0.75	3.03×10^{-4}	38	7160	1.5×10^{-4}	0.79	0.85	9.12×10^{-5}	127	4.8×10^{-4}
AN	14.9	17.2	1568	7×10^{-3}	0.66	0.31	1.13×10^{-3}	10	3970	1.9×10^{-3}	0.71	0.61	3.74×10^{-4}	31	1.2×10^{-4}

£, $, #, *(see Dabestani and Ivanov (26) and literature there cited, as well as from Notre Dame Radiation Laboratory: http://www3.nd.edu/~ndrlrcdc/.

Table 2: Quantum yields of formation (φ_{form}) and HPLC retention times (t_r) of some BaAN (**I–III**) and AN (**VIII–XIV**) photoproducts. Data obtained by HPLC. The determination of their absolute formation rates was achieved with analytical standards to calibrate the instrument.

Compound ID	t_r, min	water/ACN (70/30) φ_{form}	cyclohexane φ_{form}
I	30.5	1.5×10^{-4}	3.67×10^{-6}
II	23.7	6.9×10^{-5}	1.04×10^{-5}
III	9.0	6.25×10^{-5}	2.93×10^{-6}
VIII	8.6	8.33×10^{-4}	3.57×10^{-6}
IX	2.7	4.48×10^{-5}	4.6×10^{-7}
X	6.4	1.46×10^{-5}	1.22×10^{-6}
XI	10.1	1.14×10^{-5}	1.22×10^{-6}
XIV	55.3	ND	1.13×10^{-6}

achieved by use of suitable standards. In addition, GC/MS analyses were carried out. Photolysis was investigated in cyclohexane and in a polar solvent system consisting of an aqueous mixture of 30% ACN, to get higher concentrations of PAHs and their photoproducts, due to the very low solubility in pure water (22,23).

Photodegradation of BaAN

Photolysis in Polar Solvent. The photogenerated hydroxy BaAN derivative in the presence of O_2 should strongly absorb at approximately 300–400 nm and 220 nm (23). Literature reports indicate also that BaAN photolysis in an aqueous medium originates from the excited BaAN triplet (22). Thus, the energy transfer from the triplet state to O_2 to form singlet oxygen could result in oxidized BaAN derivatives via an endoperoxide intermediate as supposed by Jang and McDow (24), in a process that is similar to that of AN photolysis (1). Indeed, according to literature (7), 7,12-Benz[*a*]anthraquinone (**I**) is the main photoproduct obtained from aqueous samples (see Scheme 1, Table 2). Figure 2 in supplementary data shows changes in the absorption spectra of BaAN in a polar solvent system under UVA irradiation. The main peaks in the 240–300 nm range become less structured and decrease in intensity.

Figure 3 in supplementary data shows the HPLC chromatogram of a BaAN sample that has been irradiated in an aqueous solvent. This chromatogram shows the peaks of the starting compound ($t_r = 42.5$) and its photoproducts (see Tables 1 and 2 for the respective quantum yields and other kinetics parameters). As reported above, most of the products may consist of highly oxidized compounds, such as aromatic ketones, acids and anhydrides (24,25). The most

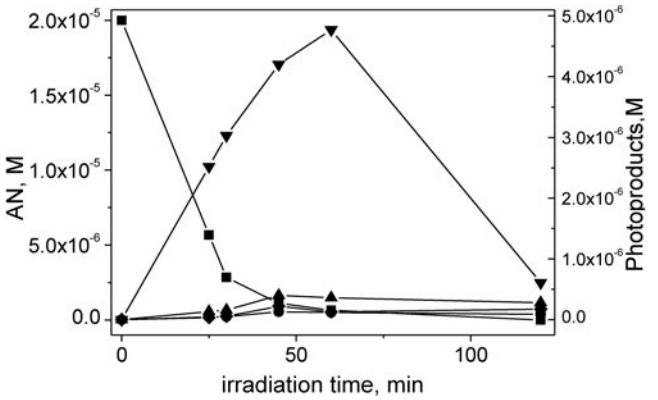

Figure 2: UVA induced photolysis s of 20 μM AN (-■-) in H_2O/ACN (70/30) at various irradiation times; XI (-♦-), IX (-▲-), VIII (-▼-), X (-●-). HPLC data.

reactive sites of BaAN are the 7 and 12 positions, so the main reaction products are 7,12-benz[*a*]anthraquinone (**I**) and 7,12-dihydroxybenz[*a*]anthracene **(II)**. According to the literature and by comparison with standards, **I** ($t_r = 30.5$) is the most abundant photoproduct obtained; the signal at $t_r = 23.7$ is due to **II**. The peak at $t_r = 9.0$ is attributed to benz[*a*]oxanthrone (**III**), which is a tautomer of **II** (7). Kinetics of BaAN photodegradation and its photoproducts formation are shown in Figure 1.

The novelty in this investigation is clearly found in the detection and characterization of several new products, using GC/MS (Figure 4 in supplementary data). The tentatively identified products are **IV** ($t_r = 21.5$) and **V** ($t_r = 22.5$). These derivatives elute after the parent compound ($t_r = 21.0$). Compound **IV** is tentatively identified as a fragment of BaAN, which is the diphenyl derivative, 1,2,3,4-tetramethyl-5-(2,3,4,5-tetramethylbenzyl)benzene. **V** shows the same fragmentation pattern and seems to be an isomeric form of **IV**. Kinetic trend (Figure 5 in supplementary data) shows that these compounds are detected only after prolonged irradiation. Thus, it is reasonable that they are photolysis products of **III** via a loss of a whole aromatic ring (Scheme 1). To confirm this statement, 5 μM solutions of **III** were irradiated up to 50 min and analyzed by GC. GC results confirm formation of photoproducts **IV** and **V** under UVA irradiation of **III**.

Photolysis in Apolar Solvent. The literature also reports that the main photoproducts of BaAN photolysis in apolar solvents are hydroxylated derivatives. BaAN photolysis in apolar media is initiated by both excited triplet and singlet states (22,23). Thus, the energy transfer from the BaAN triplet to O_2 can also oxidize BaAN to the 7,12-quinone derivative (**I**), which is the major photoproduct obtained from aqueous samples (7). The UVA-induced changes

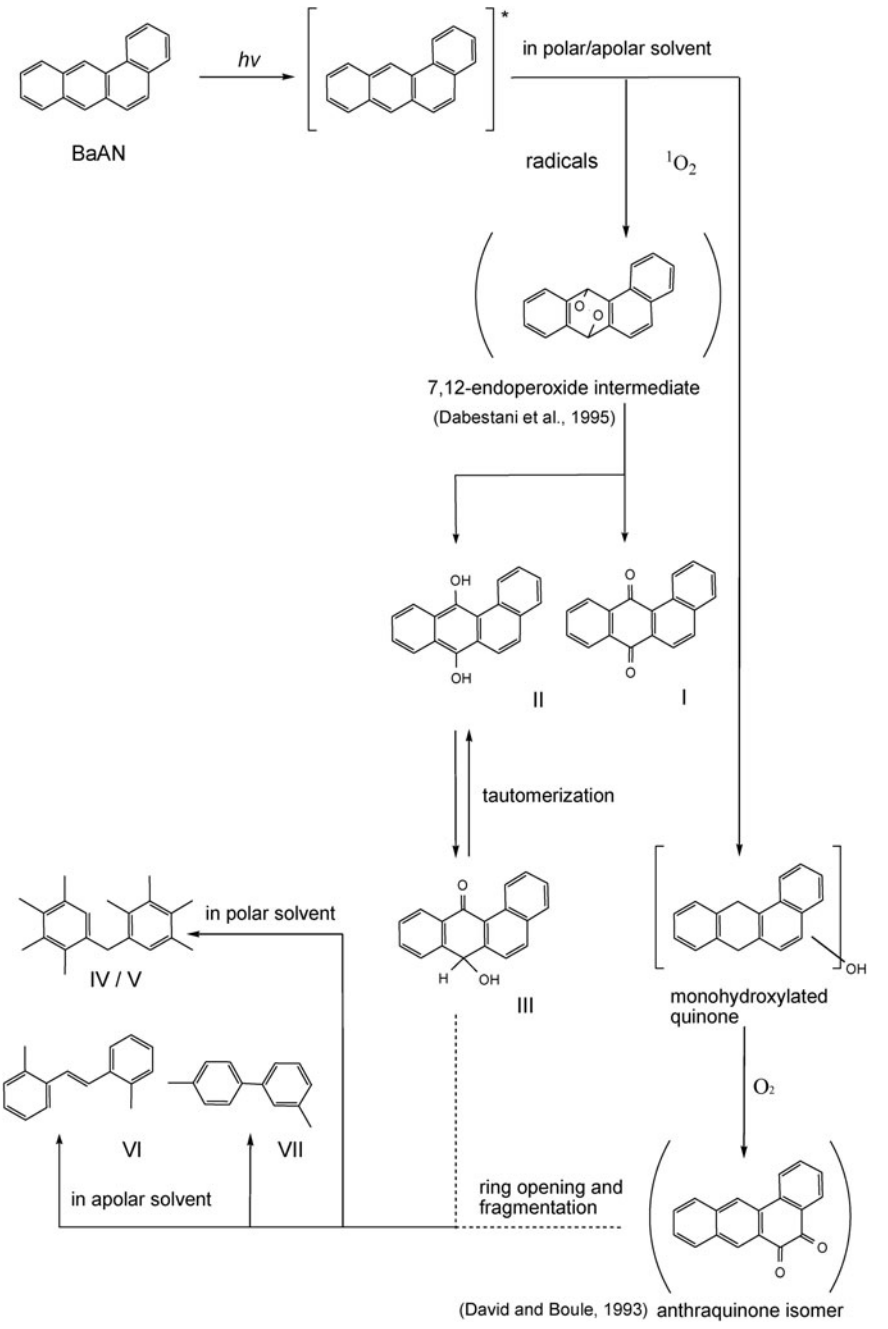

Scheme 1: BaAN photolysis.

in the BaAN absorption spectra in cyclohexane are shown in Figure 6 in supplementary data. In contrast to the aqueous media, only a decrease of the intensity in the 240–300 nm range occurs with no significant change in the peak profile. As in the case of irradiated aqueous samples, HPLC analysis of the irradiated BaAN samples shows the peaks of the starting compound and its photoproducts **I–III** (Table 2, Scheme 1, and Figure 7 in supplementary data).

Also in this case, other new products were found and characterized using GC/MS (Figure 8 in supplementary data). These derivatives elute before the parent PAH and are denoted as **VI** and **VII**. **VI** ($t_r = 5.2$) exhibits a very small molecular ion peak at 208 amu and was tentatively identified as a biphenyl form of BaAN, 1-methyl-2-[(E)-2-(2-methylphenyl)ethenyl]benzene. **VII** ($t_r = 9.4$) was tentatively identified as another biphenyl form of BaAN, 4,4′-dimethylbiphenyl. Kinetic trend (Figure 8 in supplementary data) suggests that compounds **VI** and **VII** can originate from the oxygenated photoproducts only after prolonged irradiation. Indeed, also in this case irradiation of 5 μM solutions (up to 100 min) of **III** was also performed in the same manner as for polar solvent. It results that **VI** and **VII** are photolysis products of **III** via a loss of a whole aromatic ring, as described in polar media (Scheme 1).

Photodegradation of AN

Photolysis in Polar Solvent. In UVA-induced AN photolysis in a polar solvent system we observed an increase in the absorbance at 220 nm and in the 270–300 nm range, whereas there is a decrease in the peak absorption at 250 nm and in the 300–400 nm range (Figure 9 in supplementary data). These absorption changes are likely due to the photoinduced formation of a hydroxy AN derivative in the presence of O_2 (11). In aqueous medium, approximately 70% of AN photolysis originates from the excited AN triplet (22). Thus, energy transfer from the triplet to O_2 results mainly in oxidized AN derivatives and produces to the main photoproduct, 9,10-anthraquinone (**VIII,** see Scheme 2, Table 2), via an endoperoxide intermediate that was previously observed in other solvents (1).

HPLC chromatogram peak data of AN and its photoproducts are reported in Tables 1 and 2. According to the literature (7), **VIII** is the main photoproduct ($t_r = 8.6$) in an aqueous/ACN mixture; another peak represents the hydroxy derivative of AN (**IX**, $t_r = 2.7$, Scheme 2). The peak at $t_r = 6.4$ is attributed to 9-anthrone (**X**), which is a tautomer of 9-anthranol (**XI**, $t_r = 10.1$) (Figure 2). In this figure, it is evident how these two latter compounds can originate from the major photoproduct **VIII**.

Compounds **XII** and **XIII** ($t_r = 12.5$ and 8.4, respectively) represent the new photoproducts that were never found previously in this PAH photodegradation. Indeed, formation of these compounds was evidenced in polar medium via GC/MS traces. They can represent the final fate of ring opening and

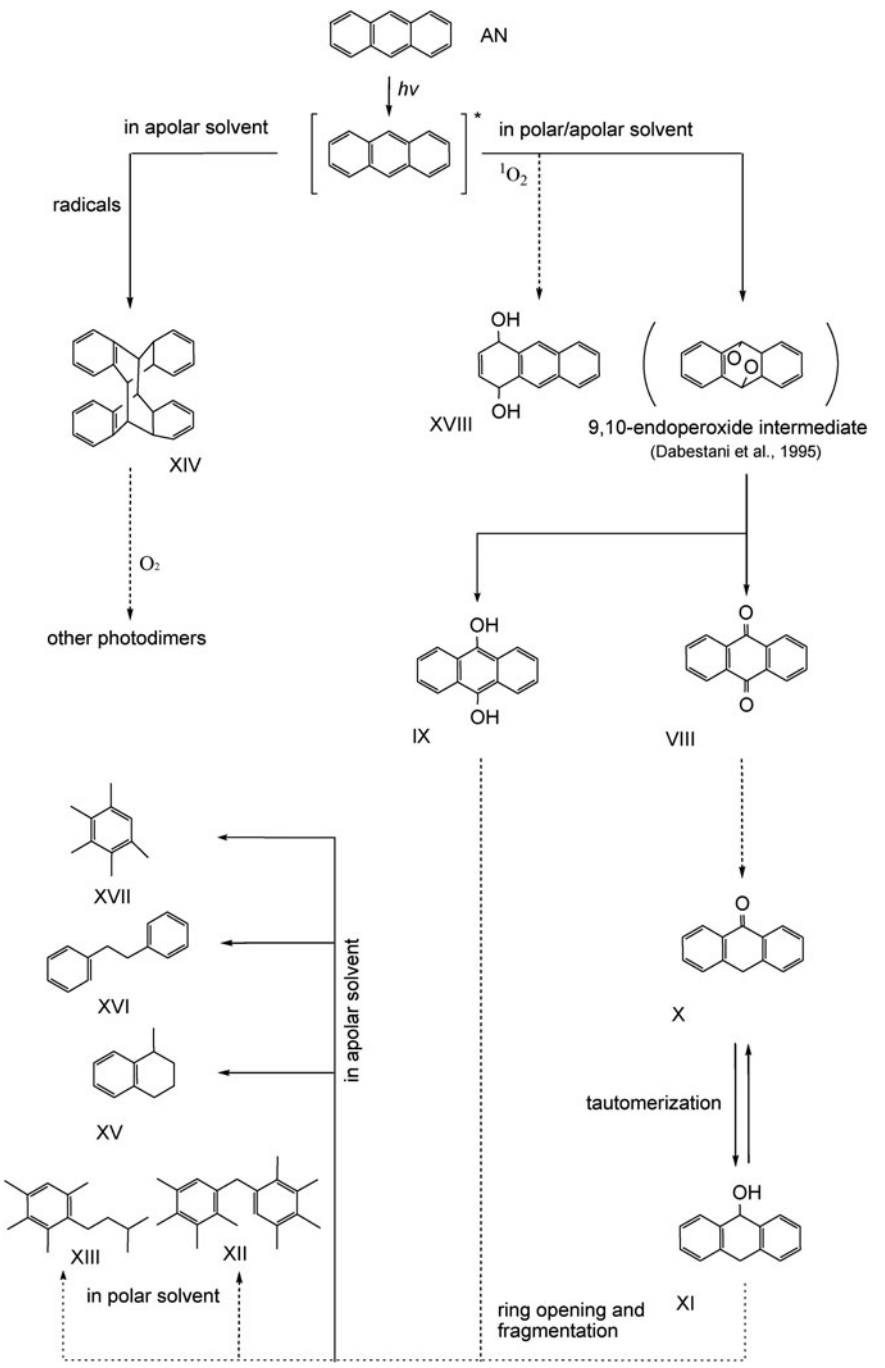

Scheme 2: AN photolysis.

fragmentation of products **IX** and **XI**. They elute before AN. **XII** was tentatively identified as a benzene fragment of AN, 1,2,3,4-tetramethyl-5-(2,3,4,5-tetramethylbenzyl)benzene. **XIII** appears to be a fragment of AN and is consistent with an aromatic moiety. Additional experiments were made in order to confirm this statement. Indeed, irradiation up to 30 min of 5 μM solutions of **IX** or **XI** gave both **XII** and **XIII**. Thus, **XII** and **XIII** are found only at longer irradiation times and can be considered the final degradation products (Figure 10 in supplementary data and Scheme 2).

Photolysis in Apolar Solvent. Figure 11 in supplementary data shows UV spectral changes for AN photodegradation in cyclohexane. AN photodimerization occurs from the excited AN singlet; in addition, reaction from the singlet state with O_2 can result, to a lesser extent, in oxidized AN derivatives (1). However, the main pathway of AN photooxidation is initiated from the triplet state (22) and produces **VIII** as the main photoproduct. The literature also reports the formation of a 9,10-photodimer (**XIV**) as a minor photoproduct in this environment (1), although it becomes the major product in deoxygenated apolar solvent system (Scheme 2).

Analogously to the photolysis in polar solvent, the formation of photoproducts **VIII**, **IX**, **X**, and **XI** was identified in all of the irradiated AN solutions (Figure 12 in supplementary data). HPLC analysis also shows the formation of the 9,10-photodimer (356 amu, **XIV**) as a minor photoproduct (1) (Figure 13 in supplementary data).

Other new photoproducts of AN in the apolar medium are observed in GC/MS traces and tentatively identified as apolar compounds (**XV–XVIII,** Scheme 2). **XV** ($t_r = 5.1$) is tentatively identified as a naphthalene fragment of AN, 1-methyltetralin. **XVI** ($t_r = 9.2$) eluted before its parent and was tentatively identified as a dibenzyl fragment of AN. **XVII** ($t_r = 16.2$) was tentatively identified as benzene residue of AN, pentamethylbenzene. These three photoproducts originate probably from fragmentation of products **IX** and **XI** via ring opening and are found only at longer irradiation times. Analogously to polar solvent experiments, formation of **XV–XVII** was confirmed by irradiating 5 μM solutions of **IX** or **XI** up to 90 min.

XVIII ($t_r = 14.5$) elutes just before AN ($t_r = 14.9$). Compound **XVIII** was tentatively identified as 1,4 dihydroxy-AN and is produced via a parallel pathway, as confirmed by kinetic data (Figure 13 in supplementary data and Scheme 2).

Comparison BaAN and AN Photodegradation in Polar and in Apolar Medium

A comparison of PAH photoreactivity in the two investigated systems must take into account that the reaction rates can be influenced by the medium polarity (films of water, composition of particulate matter, etc.) and this may affect the way and the rate through which organic compounds are processed in

the atmosphere. Moreover, a relative polar organic solvent like ACN is necessary in order to prevent PAH binding to glass surface. The substitution of an organic solvent with water is not accompanied by substantial spectral changes, as the aqueous content increases from 0% up to 70% (data not shown). With this aim, the relative relevance of our ACN/aqueous model to aqueous or wet systems was ascertained by repeating the photolysis experiments changing the ACN content. Indeed, PAHs photolysis in samples with increasing ACN content (30%, 40%, and 50%) leads to a decrease of the quantum yield. Indeed, it resulted that the quantum yield decreases from 7 to 4×10^{-3}. Experiments were carried out within 15% AN photodegradation (5 min irradiation of a 20 μM solution). Similar experiments were carried out with BaAN. Thus, 45 min irradiation of a 4.4 μM BaAN solution shows a decrease from 4.2 to 0.6×10^{-4}. This can be considered in good agreement with the reported effect of solvent polarity on PAHs photochemistry (13,22,23).

According to the literature, quinones are the main photoproducts of BaAN and AN in aqueous media in aqueous media, and hydroxy derivatives are also found, but in lower amounts (7,22). These compounds were also found after photolysis in apolar media, but in this case, the photochemical process tends to favor the formation of other photoproducts, for example AN dimer (XIV, Table 2). The new aspect of this picture is provided by the study of the photoreactivity of previously identified photoproducts, that when accumulate absorb light, giving rise, both in polar and apolar medium, to new photochemical paths (mainly fragmentations) described in the previous section. Apart from differences in the photophysical behaviors, there is a substantial difference in the UVA photochemical reactivity between BaAN and AN. The latter is more susceptible to photolysis than BaAN, as shown in Table 1, which lists the degradation parameters of the compounds based on k, $t_{1/2}$ and quantum yields. Taking into account (values in Table 1):

a. the matching UVA light absorption rates of AN and BaAN;
b. the Inter System Crossing quantum yields;
c. the singlet oxygen lifetimes; and
d. the reaction rate constants in organic solvents of AN and BaAN with singlet oxygen.

We can infer that the singlet oxygen production, is the prominent, but not the only one, pathway involved in the general scheme of PAH photolysis both in polar and apolar environments, as confirmed by previous literature. Indeed, it was previously suggested that BaAN is largely photodegraded via photoionization, whereas energy transfer from excited triplet is relevant to AN photolysis (22,23)

Thus, additional experiments carried out in nitrogen saturated solvents resulted in a slower photodegradation, more evident for AN (3.7 vs. 0.9×10^{-4}) respect to BaAN (9.1 vs. 3.9×10^{-5}). This fact corroborates the role played by oxygen, also if the radical pathway influences PAH photodegradation, as demonstrated by the drastic reduction of primary photoproducts, more significant in the case of AN.

The relative photostability of BaAN, as results from the values of photodegradation rate constants in both solvent systems, can be explained by the electronic configuration of these two compounds. PAHs are susceptible to oxidation at the position in which frontier electron density is high (27). This latter is higher in the case of the 9 and 10 positions of AN compared to the 7 and 12 positions of BaAN (28). Indeed, angular BaAN is more resistant to photodecomposition than linear AN. It appears that both excited states of PAHs can form stable pairs, i.e. a charge transfer complex, with molecular oxygen (22).

The main photochemical pathways of BaAN and AN in aqueous (23) and apolar (24) media are known, but this paper sheds more light on new photoproducts (Schemes 1 and 2). The reactions proceed until complete degradation has occurred (Figures 1 and 2).

In an aqueous solvent, the excited PAH singlet is more reactive with O_2 compared to the triplet state (22). Photoionization proceeds mainly through electron transfer to produce PAH^+, whereas the PAH triplet reacts directly with O_2. The data in the literature suggest that BaAN is largely photodegraded via the former pathway, whereas the latter mechanism is relevant to AN photolysis (22, 23). Indeed, PAH photolysis seems to be controlled mainly by the lifetime and the reactivity of the excited singlet (22,23). The difference in reactivity between AN and BaAN could be due to the hydrogen donor potential of the solvents and the stability of the resulting solvent radicals (12). In summary, photolysis quantum yields and reaction rate constants show that AN is less photostable than BaAN, and the photostability of both compounds is lower in polar media than apolar media (Table 1). The PAH photodegradation and some of their photoproducts formation parameters are of the same order of magnitude as those reported in the literature (12,13,22,23,29). The nature and intensity of light sources used, as well as solvent type and ratio can easily explain some differences. For example, BaAN irradiation carried out in aqueous solvent, with 1% ACN and a filtered 400 W medium pressure mercury lamp to give 366 nm band, gave a $k = 1.3 \times 10^{-4}$ s^{-1} (29), whereas the k was 6.1×10^{-5} s^{-1} in cyclohexane with a Pyrex filtered 450 W high-pressure mercury lamp (12). Plata et al. (13) calculated 6.2×10^{-5} in toluene and a UVB filtered 300W xenon lamp. Rate constant for AN in polar solvent (water-0.5% ACN, 300W Xe arc lamp 305 nm filtered) was 1×10^{-3} s^{-1} (22).

The characterization of the new photoproducts helps clarify the involved photochemical pathways (Scheme 1 and 2).

Meanwhile, in a single component model system there are some limitations in representing aerosol phase reactions. In particular, the aerosol phase contains very complex organic matter and high concentrations of inorganic ions, both of which are known to affect photodegradation rates and reaction products (25). Moreover, there are some factors that can influence PAH photodegradation in atmospheric PM heterogeneous reactions (30–32). The structure of the PAH influences the heterogeneous reactivity towards oxidation, as well as, the conditions of particles loading and the nature of the particles. Graphite particles stabilize the most reactive PAHs towards oxidation, also if particle size is known to be non influent towards these kinds of reactions (30–32). Moreover, pore size, as well as surface area may influence local PAH concentration in particulate matter and consequently, their reactivity. This justifies heterogeneous reactions of PAHs as processes relevant from an atmosphere point of view (30).

On the other hand, lab-simulated environmental PAH photolysis minimizes environmental complications, thus achieving a reproducible product distribution and isolating the mechanism investigated in the present study. Hence, the obtained results should help explain PAH photolysis under real conditions, which are encountered in the atmosphere, where several parameters influence the photochemistry. In addition, identification of new photofragmentation paths, originating by irradiation of primary PAH photoproducts, may suggest an innovative way of remediation triggered by light.

FUNDING

We gratefully acknowledge financial support from MIUR, Roma, Italy, PRIN2009.

REFERENCES

1. Dabestani, R., K. J. Ellis, and M. E. Sigman. “Photodecomposition of Anthracene on Dry Surfaces: Products and Mechanism.” *Journal of Photochemistry and Photobioliology A: Chemistry* 86 (1995): 231–239.

2. Dabestani, R. and M. E. Sigman. “Phototransformation of Polycyclic Aromatic Hydrocarbons (PAHs) on a Non-Semi Conductive Surface such as Silica,” 3. *International Conference on TiO, Photocatalytic Purification and Treatment of Water and Air*, Orlando, 1997.

3. Motta, S., V. Librando, Z. Minniti, C. Federico, and S. Saccone. “Identification of Genotoxic Compounds in the Airborne Particulate Matter Endowed by Small Aerodynamic Diameter in the City of Catania (Italy).” *Annali di Chimica* 96 (2006): 537–542.

4. Librando, V., G. Tomaselli, and G. Tringali. “Optimization of Supercritical Fluid Extraction by Carbon Dioxide with Organic Modifiers of Polycyclic Aromatic Hydrocarbons from urban particulate matter.” *Annali di Chimica* 95 (2005): 211–216.

5. Librando, V. and G. Tringali. "Atmospheric Fate of OH Initiated Oxidation of Terpenes. Reaction Mechanism of Alpha-Pinene Degradation and Secondary Organic Aerosol Formation." *Journal of Environmental Management* 75 (2005):275–282.

6. Kahan, T. F. and D. J. Donaldson. "Photolysis of Polycyclic Aromatic Hydrocarbons on Water and Ice Surfaces." *The Journal of Physical Chemistry A* 111 (2007): 1277–1285.

7. David, B. and P. Boule. "Phototransformation of Hydrophobic Pollutants in Aqueous Medium I- PAHs Adsorbed on Silica." *Chemosphere* 26 (1993):1617–1631.

8. Pagni, R. M., and R. Dabestani. "Recent Developments in the Environmental Phorochemistry of PAHs and PCBs in Water and on Solids." *The Handbook of Environmental Chemistry* 2 (2005):193–219.

9. Beltran, F. J., M. Gonzalez, and J. Rivas. "Advanced Oxidation of Polynuclear Aromatic Hydrocarbons in Natural Waters." *Journal of Environmental Science and Health A* 31 (1996): 2193–2210.

10. Beltran, F. J., G. Ovejero, and J. Rivas. "Oxidation of Polynuclear Aromatic Hydrocarbons in Water. 4. Ozone Combined with Hydrogen Peroxide." *Industrial & Engineering Chemistry Research* 35 (1996):883–890.

11. Dabrowska, D., A. Kot-Wasik, and J. Namiesnik. "Stability Studies of Selected Polycyclic Aromatic Hydrocarbons in Different Organic Solvents and Identification of Their Transformation Products." *Polish Journal of Environmental Studies* 17 (2008): 17–24.

12. Ohura, T., T. Amagai, and M. Makino. "Behavior and Prediction of Photochemical Degradation of Chlorinated Polycyclic Aromatic Hydrocarbons in Cyclohexane." *Chemosphere* 70 (2008):2110–2117.

13. Plata, D. L., C. M. Sharpless, and C. M. Reddy. "Aromatic Hydrocarbons in Oil Films." *Environmental Science & Technology* 42 (2008):2432–2438.

14. Zheng, B., H. Hwang, H. Yu, and S. Ekunwe. "DNA Damage Produced in HaCaT Cells by Combined Fluoranthene Exposure and Ultraviolet A Irradiation." *Environmental and Molecular Mutagenesis* 44 (2004):151–155.

15. Finalayson-Pitts, B. J. and J. N. Pitts. "Tropospheric Air Pollution: Ozone, Airborne Toxics, Polycyclic Aromatic Hydrocarbons, and Particles." *Science* 276 (1997): 1045–1051.

16. Librando, V., G. Tringali, J. Hjorth, and S. Coluccia. "OH-initiated Oxidation of DMS/DMSO: Reaction Products at High NOx Levels." *Environmental Pollution* 127 (2004):403–410.

17. Chen, J., F. S. Ehrenhauser, K. T. Valsaraj, and M. J. Wornat. "Uptake and UV-Photooxidation of Gas-Phase PAHs on the Surface of Atmospheric Water Films. 1. Naphthalene." *The Journal of Physical Chemistry A* 110 (2006):9161–9168.

18. Sumner, A.L., E. J. Menke, Y. Dubowski, J. T. Newberg, R. M. Penner, J. C. Hemminger, L. M. Wingen, T. Brauers, and B. J. Finlayson-Pitts. "The Nature of Water on Surfaces of Laboratory Systems and Implications for Heterogeneous Chemistry in the Troposphere." *Journal of Physical Chemistry Chemical Physics* 6 (2004):604–613.

19. Lehto, K.-M., E. Vuorimaa, and H. Lemmetyinen. "Photolysis of Polycyclic Aromatic Hydrocarbons (PAHs) in Dilute Aqueous Solutions Detected by Fluorescence." *Journal of Photochemistry and Photobiology A: Chemistry* 136 (2000):53–60.

20. Calvert, G. and J. Pitts. "Experimental Methods in Photochemistry." In *Photochemistry*, eds. G. Calvert and J. Pitts (New York: Wiley, 1966):783–786.

21. Giammona, G., G. Pitarresi, V. Tomarchio, G. De Guidi, and S. Giuffrida. "Swellable Microparticles Containing Suprofen: Evaluation of in vitro Release and Photochemical Behaviour." *Journal of Controlled Release* 51 (1998): 249–257.

22. Fasnacht, M. P. and N. Blough. "Mechanisms of the Aqueous Photodegradation of Polycyclic Aromatic Hydrocarbons." *Environmental Science & Technology* 37 (2003): 5767–5772.

23. Fasnacht, M. P. and N. V. Blough. "Kinetic Analysis of the Photodegradation of Polycyclic Aromatic Hydrocarbons in Aqueous Solution." *Aquatic Sciences* 65 (2003): 352–358.

24. Jang, M. and S. R. McDow. "Products of benz[a]anthracene Photodegradation in the Presence of Known Organic Constituents of Atmospheric Aerosols." *Environmental Science & Technology* 31 (1997): 1046–1053.

25. Jang, M. and S. R. McDow. "Benz[a]anthracene Photodegradation in the Presence of Known Organic Constituents of Atmospheric Aerosols." *Environmental Science & Technology* 29 (1995): 2654–2660.

26. Dabestani, R., and I. N. Ivanov. "A Compilation of Physical, Spectroscopic and Photophysical Properties of Polycyclic Aromatic Hydrocarbons." *Photochemistry* and Photobiology 70 (1999): 10–34.

27. Lee, B. D., M. Iso, and M. Hosomi. "Prediction of Fenton Oxidation Positions in Polycyclic Aromatic Hydrocarbons by Frontier Electron Density." *Chemosphere* 42 (2001): 431–435.

28. Low, G. K. C., G. E. Batley, and C. I. Brockbank. "Solvent-Induced Photodegradation as a Source of Error in the Analysis of Polycyclic Aromatic Hydrocarbons." *Journal of Chromatography* 392 (1987): 199–210.

29. Mill, T., W. R. Mabey, B. Y. Lan, and A. Baraze. "Photolysis of polycyclic Aromatic Hydrocarbons in Water." *Chemosphere* 10 (1981): 1281–1290.

30. Perraudin, E., H. Budzinski, and E. Villenave. "Kinetic Study of the Reactions of Ozone with Polycyclic Aromatic Hydrocarbons Adsorbed on Atmospheric Model Particles." *Journal of Atmospheric Chemistry* 56 (2007): 57–82.

31. Wild, E., J. Dent, G. O. Thomas, and K. C. Jones. "Real-Time Visualisation and Quantification of PAH Photodegradation on and within Plant Leaves." *Environmental Science & Technology* 39 (2005): 268–273.

32. Lihong, Z., L. Peijun, G. Zongqiang and L. Xuemei. "Photocatalytic Degradation of Polycyclic Aromatic Hydrocarbons on Soil Surfaces using TiO2 under UV light." *Journal of Hazardous Material* 158 (2008): 478–484.